

NUMERICAL STUDY OF THE MICROBUNCHING INSTABILITY AT UVSOR-III: INFLUENCE OF THE RESISTIVE AND INDUCTIVE IMPEDANCES

E. Roussel*, C. Evain, C. Szwaj, S. Bielawski, PhLAM, Villeneuve d'Ascq, France

J. Raasch, P. Thoma, A. Scheuring, K. Ilin, M. Siegel, KIT, Karlsruhe, Germany

M. Hosaka, N. Yamamoto, Y. Takashima, Nagoya University, Nagoya, Japan

H. Zen, Kyoto University, Kyoto, Japan,

T. Konomi, M. Adachi, S. Kimura, M. Katoh, UVSOR, Okazaki, Japan

Abstract

At high charge, relativistic electron bunches circulating in storage rings undergo an instability, the so-called microbunching or the CSR (Coherent Synchrotron Radiation) instability. This instability is due to the interaction of the electrons with their own radiation and leads to the formation of microstructures (at millimeter scale) in the longitudinal phase space. Here we present results of the modeling of the dynamics at UVSOR-III using a one dimensional Vlasov-Fokker-Planck equation. In particular, we focus on the effect of impedance (such as the shielded CSR impedance but also the resistive and inductive impedances) and noise on the CSR dynamics.

INTRODUCTION

In a relativistic electron bunch, the interaction of the electrons with their own electromagnetic field (walefield) can induce the so-called “microbunching instability” [1–3] which is characterized by the spontaneous formation of patterns in the electron bunch phase-space at a millimeter scale. This effect has been observed and studied in various storage ring facilities such as ALS [3], ANKA [4], BESSY [5], DIAMOND [6], ELETTRA [7], MLS [8], Synchrotron SOLEIL [9] and UVSOR [10]. Recently, direct recordings of the bunch microstructure dynamics using ultra-fast detectors based on superconducting thin film YBCO have been reported [11]. These experimental data provide a severe test for numerical models of the CSR instability. Here we present results of the modeling of the dynamics at UVSOR-III using a one dimensional Vlasov-Fokker-Planck equation. In particular, motivated by the asymmetry of the bunch profile, we study the effect of several types of impedance such as the shielded CSR impedance but also the resistive and inductive impedances.

LONGITUDINAL BEAM DYNAMICS

Vlasov-Fokker-Planck equation

For the numerical simulation we use the Vlasov-Fokker-Planck (VFP) equation [1] to describe the evolution of the electron density distribution function $f(q, p, \theta)$ in the longitudinal phase-space (q, p) , where q , p and θ are the longitudinal position, relative momentum and time (dimensionless

variables).

$$\frac{\partial f}{\partial \theta} - p \frac{\partial f}{\partial q} + \left[q - I_c E_{wf}(q) - \frac{2\langle p \rangle}{\omega_s \tau_R} \right] \frac{\partial f}{\partial p} = 2\epsilon \left[f(q, p, \theta) + p \frac{\partial f}{\partial p} + \frac{\partial^2 f}{\partial p^2} \right] \quad (1)$$

$I_c E_{wf}(q)$ is the collective force due to the interaction between the electrons and their own radiation. The term $-\frac{2\langle p \rangle}{\omega_s \tau_R}$ represents the Robinson damping with ω_s the synchrotron frequency and τ_R the Robinson damping time.

Longitudinal Impedances

Concerning the wakefield term, we consider an electron moving on a circular orbit between two parallel plates (shielded CSR wakefield) [12] and we have added the resistive R and inductive L impedances [13] to take into account a global effect due to the complex vacuum chamber geometry.

$$E_{wf}(q) = \frac{eN_e}{\sigma_z/c} R \rho(q) - \frac{eN_e}{(\sigma_z/c)^2} L \frac{\partial \rho}{\partial q} + N_e \int_{-\infty}^{+\infty} E_{CSR}(q - q') \rho(q') dq' \quad (2)$$

Since the real electron bunch distribution function is not smooth due to the granularity of the electrons, a white noise term is adding to the electron bunch density $\rho_0(p, q)$ at each step of VFP integration in a phenomenological way:

$$\rho(q, \theta) = \rho_0(q, \theta) + \frac{1}{\sqrt{N}} \sqrt{\rho_0(q, \theta)} \xi(q, \theta) \quad (3)$$

with $\xi(q, \theta)$ a Gaussian white noise and N the number of electrons in the bunch.

The resistive and inductive wakefield can induce a lengthening and distortion of the electron bunch. We estimate the value of R and L by integrating the VFP equation and try to find a bunch profile similar to the experimental bunch profile, as illustrated in figure 1.

The parameters used in the numerical simulations are summarized in the table 1.

NUMERICAL RESULTS

Shielded CSR Impedance

In a first step, only the shielded CSR impedance is taken into account. The figure 2 illustrates the link between the

05 Beam Dynamics and Electromagnetic Fields

D05 Instabilities - Processes, Impedances, Countermeasures

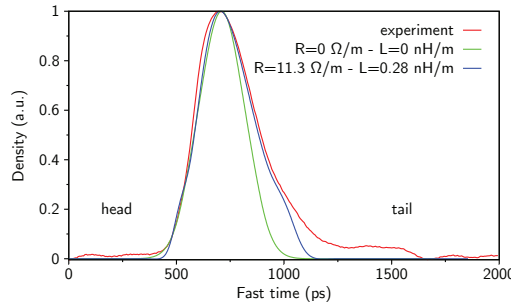


Figure 1: Average longitudinal electron bunch profile on the UVSOR-III storage ring above the instability threshold. (red: experiment at $I = 62$ mA, green: numerical simulation without R and L wakefields and blue: numerical simulations with R and L wakefields at $I = 120$ mA). Note that each density is normalized such that the maximum is equal to 1.

Table 1: UVSOR-III storage ring parameters

Nominal Energy E_0 (MeV)	600
Momentum Compaction Factor α_0	0.033
Circumference C (m)	53.2
Relative Energy Spread σ_δ	$4.36 \cdot 10^{-4}$
Natural Bunch Length σ_z (cm)	3
Revolution Period T_0 (ns)	177
Bending Radius R_c (m)	2.2
Vacuum Chamber Height $2h$ (cm)	3.8
Synchrotron Frequency f_s (kHz)	23.1
Synchrotron Damping Time τ_s (ms)	32.36
Resistive Impedance R (Ω /m)	11.3
Inductive Impedance L (nH/m)	0.28
Robinson Damping Time τ_R (μ s)	43.2

longitudinal electron bunch phase-space [Fig. 2(a)] and the CSR electric field [Fig. 2(c)] emitted during the microbunching instability. Above a current threshold (here, ≈ 100 mA in the simulations), microstructures appear spontaneously in the electron bunch distribution [Fig. 2(a)]. The experimental observations of these structures can be possible by either recording the longitudinal profile of the electron bunch [Fig. 2(b)] which corresponds to the projection of the electron bunch distribution along the longitudinal position axis or recording the CSR pulses [Fig. 2(c)]. The figure 2(d) represents the temporal evolution of the CSR electric field turn-by-turn.

Note that the structures move toward the head of the bunch with a slope of 20 ps/ μ s (blue dashed lines in Fig. 2(d)).

Influence of the R and L Impedances and noise

In a second step, we take into account the effect of the resistive and inductive impedances as well as the contribution of the shot noise. Above the instability threshold, the numerical results reveal the spontaneous formation of microstructures in the electron bunch distribution function [Fig. 3(a)]. However, since we added a resistive wakefield, a larger structure is now present which wrap the whole elec-

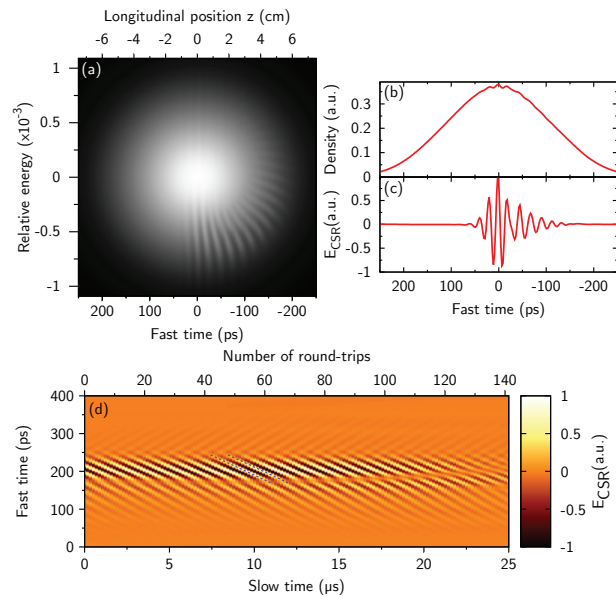


Figure 2: (a) Longitudinal electron bunch phase-space, (b) associated bunch profile and (c) associated CSR electric field. (d) Color map of the temporal evolution of the CSR pulses. (a,b,c) are taken at the beginning of (d). The beam current is $I = 120$ mA.

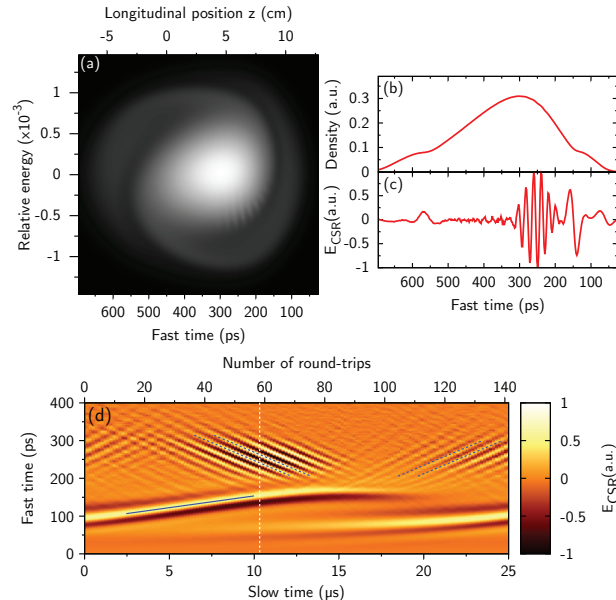


Figure 3: (a) Longitudinal electron bunch phase-space, (b) associated bunch profile and (c) associated CSR electric field. (d) Color map of the temporal evolution of the CSR pulses. (a,b,c) are taken at time $t = 10.4$ μ s (white dashed line in (d)). The beam current is $I = 120$ mA and $R = 11.3$ Ω /m and $L = 0.28$ nH/m.

tron bunch in a “spiral” shape. From the calculation of the CSR electric field [Fig. 3(c)], we notice that the spiral is at the origin of the structures at the borders of the CSR pulse whereas the thin microstructures are responsible for the fast

oscillations at the center. Because the electron bunch distribution rotates in phase-space, the structures in the CSR electric field drift along the longitudinal position, i.e. along the fast time axis [Fig. 3(d)]. The structures at the bottom are drifting toward the tail with a slope of 5.5-6.5 ps/μs (blue line in Fig. 3(d)) and the second structures move in both directions with a higher slope of 19-20 ps/μs (blue dashed line in Fig. 3(d)) which is different to the case without the resistive and inductive impedances.

CONCLUSION

We study the electron bunch dynamics using numerical simulations when under the influence of shielded CSR wake-field combined to resistive and inductive impedances. We show that R and L impedances result in a bunch lengthening and an asymmetric bunch profile. As a result, the spatiotemporal evolution of the microstructures in the bunch is strongly altered. New experimental possibilities using thin-film YBCO detector or electrooptic detection technique will allow to make severe comparisons of the models.

ACKNOWLEDGMENT

The work was supported by the Joint Studies Program of the Institute for Molecular Science, the JSPS fellowship program for research in Japan (S-09171), the Projet International de Coopération Scientifique PICS project from CNRS, the Grant-in-aid for scientific researches (B20360041) of JSPS, the ANR (Blanc 2010-042301), and used HPC resources from GENCI TGCC/IDRIS (2013-x2013057057). The CERLA is supported by the French Ministère chargé de la Recherche, the Région Nord-Pas de Calais and the FEDER. The KIT is supported in part by the German Federal Ministry of Education and Research under Grant N°05K2010.

REFERENCES

- [1] M. Venturini, R. Warnock, Phys. Rev. Lett. 89, 224802 (2002).
- [2] G. Stupakov, S. Heifets, Phys. Rev. ST Accel. Beams 5, 054402 (2002).
- [3] J. Byrd et al, Phys. Rev. Lett. 89, 224801 (2002).
- [4] V. Judin et al., “Spectral and temporal observations of CSR at ANKA”, IPAC 2012, New Orleans, June 2012, TUPPP010 (2012).
- [5] M. Abo-Bakr et al. Phys. Rev. Lett. 88, 254801 (2002).
- [6] W. Shields et al. Journal of Physics: Conference Series 357, 012037 (2012).
- [7] E. Karantzoulis et al. Infrared Physics and Technology 53, 300 (2010).
- [8] G. Wüstefeld et al. “Coherent THz measurements at the metrology light source” IPAC 2010, Kyoto, June 2010, WEP-PEA015 (2010).
- [9] C. Evain et al. Europhys. Lett. 98, 40006 (2012).
- [10] A. Mochihashi et al., “Observation of THz synchrotron radiation burst in uvsor-ii electron storage ring” EPAC06, Edinburgh, THPLS041 (2006).
- [11] E. Roussel et al., “First Direct, Real Time, Recording of the CSR Pulses Emitted During the Microbunching Instability, using Thin Film YBCO Detectors at UVSOR-III”, IPAC’14, Dresden, Germany, This Conference.
- [12] J.B. Murphy et al. Part. Accel. 57, 9 (1997).
- [13] I.P.S Martin et al., “Modelling the Steady State CSR Emission in Low Alpha Mode at the DIAMOND Storage Ring”, IPAC’12, New Orleans, TUPPP031 (2012).